PCCP

Accepted Manuscript

This is an *Accepted Manuscript*, which has been through the Royal Society of Chemistry peer review process and has been accepted for publication.

Accepted Manuscripts are published online shortly after acceptance, before technical editing, formatting and proof reading. Using this free service, authors can make their results available to the community, in citable form, before we publish the edited article. We will replace this *Accepted Manuscript* with the edited and formatted *Advance Article* as soon as it is available.

You can find more information about *Accepted Manuscripts* in the Information for Authors.

Please note that technical editing may introduce minor changes to the text and/or graphics, which may alter content. The journal's standard Terms & Conditions and the Ethical guidelines still apply. In no event shall the Royal Society of Chemistry be held responsible for any errors or omissions in this *Accepted Manuscript* or any consequences arising from the use of any information it contains.

ROYAL SOCIETY OF CHEMISTRY

www.rsc.org/pccp

NON-NEWTONIAN RHEOLOGICAL PROPERTIES OF SHEARING NEMATIC LIQUID CRYSTAL MODEL SYSTEMS BASED ON THE GAY-BERNE POTENTIAL

Sten Sarman, Yong-Lei Wang and Aatto Laaksonen
Department of Materials and Environmental Chemistry
Arrhenius Laboratory
Stockholm University
106 91 Stockholm, Sweden

Physical Chemistry Chemical Physics Accepted Manuscript

Abstract

The viscosities and normal stress differences of various liquid crystal model systems based on the Gay-Berne potential have been obtained as functions of the shear rate in the non-Newtonian regime. Various molecular shapes such as regular convex calamitic and discotic ellipsoids and non-convex shapes such as bent core molecules and soft ellipsoid strings have been examined. The isotropic phases were found to be shear thinning with the shear rate dependence of the viscosity following a power law in the same way as alkanes and other non-spherical molecules. The nematic phases turned out to be shear thinning but the logarithm of the viscosity proved to be an approximately linear function of the square root of the shear rate. The normal stress differences were found to display a more or less parabolic dependence on the shear rate in the isotropic phase whereas this dependence was linear at low to intermediate shear rates in the nematic phase.

Physical Chemistry Chemical Physics Accepted Manuscript

1. Introduction

Shear flow simulations of molecular model systems in the non-Newtonian regime have been undertaken since the 1970's when the Lees-Edwards sliding brick boundary conditions were introduced [1].Then a velocity gradient and a shear stress are built up in the system so that the viscosity can be obtained as the ratio of these two quantities. Later on this method was improved by devising the SLLOD equations of motion [2] where the molecular velocity is divided into the streaming velocity and the velocity relative to the streaming velocity or the molecular thermal velocity where the sum of the squares of the last-mentioned velocities is proportional to the temperature. At first simple liquids such as Lennard-Jones liquids were studied, but since the mid 1980's it has been possible to study shear flow of molecular liquids, such as, for example, alkanes [3]. They are of technological interest since they, among other things, are constituents of lubricants. At first united atom models were applied where the methyl or methylene groups were represented by a Lennard-Jones interaction site and where the bond lengths and bond angles were kept constant by application of Lagrangian constraints [4, 5]. Later on more detailed models with bond stretching and bond bending potentials and with explicit representation of the hydrogen atoms were introduced [6]. An interesting result of these simulations is the finding that simple liquids and linear alkanes are shear thinning. In the non-Newtonian regime the viscosity of the simple liquid is a linear function of the square root of the shear rate whereas the viscosity of the alkanes and other non-spherical molecules follows a power law at high shear rates. The reason why the alkanes are shear thinning is that the shear field is a sum of two velocity fields, namely one purely rotational field and one irrotational elongational field, where the latter field stretches out the molecules and pulls them towards the 45 degree orientation relative to the stream lines [7]. Thereby the molecules become more streamlined and they are able to pass each other more readily, so that the friction decreases. In fact a nonequililbrium nematic liquid crystal is formed. The rotational part of the velocity field exerts a torque on the molecules twisting them towards the streamlines so that the alignment angle becomes less than 45 degrees at high shear rates.

Another class of systems the flow properties of which have been studied is various liquid crystals. Most of these studies deal with simplified model systems such as the Gay-Berne fluid [8, 9], which can be regarded as Lennard-Jones fluid generalized to ellipsoidal molecular cores, even though some studies of atomistic models of 4-cyano-4'-*n*-pentylbiphenyl (5CB) are available [10]. However, with few exceptions [11] these studies deal either with the evaluation of the Green-Kubo relations for the viscosities [12, 13] or with shear flow in the Newtonian regime [14-16]. On the experimental side, most of the studies of the

Physical Chemistry Chemical Physics Accepted Manuscript

rheology of liquid crystals have been focused on the viscosities in the linear regime [17, 18] but recently there has been some works published on the viscosity in the non-Newtonian regime of nematic liquid crystals [19, 20].

Therefore, the purpose of this work is to study shear flow of molecular model systems in the nematic phase in the non-Newtonian regime. Since many lubricants form liquid crystals at high shear rates and some liquid crystals are used as lubricants or additives to lubricants [21, 22], this is also of technological interest. Various types of molecular shapes will be tested such has convex calamitic and discotic molecules, bent core molecules and soft ellipsoid strings.

The article is organized as follows: in section 2 the necessary theory is reviewed, in section 3 the model systems are described, in section 4 the technical details are given, in section 5 the results are presented and discussed and in section 6 there is a conclusion.

2. Basic theory

2.1 Order parameter

Since we are dealing with liquid crystals it is useful to introduce a scalar order parameter and a director, which is a measure of the average orientation of the molecules, since many properties of liquid crystals become simpler when they are expressed relative to a director based coordinate system. The order parameter and the director are obtained by from the order tensor,

$$\mathbf{Q} = \frac{3}{2}\left(\frac{1}{N}\sum_{i=1}^{N} \hat{\mathbf{u}}_i \hat{\mathbf{u}}_i - \frac{1}{3}\mathbf{1} \right), \tag{2.1}$$

where N is the number of molecules in the system, $\mathbf{1}$ is the unit second rank tensor and $\{\hat{\mathbf{u}}_i; 1 \le i \le N\}$ is some characteristic unit vector of the molecules. For bodies of revolution, $\hat{\mathbf{u}}_i$ can be parallel to the axis of revolution and for less regular rigid calamitic molecules it can be parallel to the axis corresponding to the smallest eigenvalue of the inertia tensor. The largest eigenvalue of the order tensor is defined as the order parameter S. When the molecules are perfectly aligned in the same direction the order parameter is equal to unity and when the orientation is completely random it is equal to zero. The director $\mathbf{n}$ is the eigenvector corresponding to the order parameter. In terms of the director and the order parameter the order tensor may also be expressed as

$$\mathbf{Q} = \frac{3}{2} S\left(\mathbf{nn} - \frac{1}{3}\mathbf{1} \right). \tag{2.2}$$

Physical Chemistry Chemical Physics Accepted Manuscript

Usually the director is not fixed in space but it diffuses on the unit sphere with an angular velocity given by

$$\boldsymbol{\Omega} = \mathbf{n} \times \dot{\mathbf{n}} \,. \tag{2.3}$$

The order parameter and the director are functions of the position in space in a macroscopic system, but in this work we will be interested simulations cells which are small systems where these quantities are the same over the whole system

2.2 Equations of motion

In order to study shear flow and to calculate the viscosity in the non-Newtonian regime, the SLLOD equations of motion are applied [2]. In the case of rigid molecules they take the following form in linear space:

$$\dot{\mathbf{r}}_i = \frac{\mathbf{p}_i}{m} + \gamma r_{zi} \mathbf{e}_x \tag{2.4a}$$

and

$$\dot{\mathbf{p}}_i = \mathbf{F}_i - \gamma p_{zi} \mathbf{e}_x - \xi \mathbf{p}_i \,, \tag{2.4b}$$

where $\mathbf{r}_i$ and $\mathbf{p}_i$ are the position and peculiar momentum, *i.e.* the momentum relative to the streaming velocity, of molecule *i*, *m* is the molecular mass, $\gamma = \partial u_x / \partial z$ is the shear rate, *i. e.* there is a streaming velocity u_x in the *x*-direction varying linearly in the *z*-direction, $\mathbf{e}_x$ is the unit vector in the *x*-direction, $\mathbf{F}_i$ is the force exerted on molecule *i* by the other molecules and ξ is a Gaussian thermostatting multiplier given by the constraint that the linear peculiar kinetic energy should be a constant of motion,

$$\xi = \frac{\sum_{i=1}^{N} \left[\mathbf{F}_i \cdot \mathbf{p}_i - \gamma p_{ix} p_{iz} \right]}{\sum_{i=1}^{N} \mathbf{p}_i^2} \,. \tag{2.5}$$

Note that when this thermostat is applied it is assumed that there is a linear velocity profile. This is a reasonable assumption if the shear rate is not too high, which is the case in most experimentally relevant situations, where the equipartitions principle is still valid, and in the simulations in the present work. However, if state points far from equilibrium, where the flow is turbulent, are studied other kinds of thermostats must be used, where there are no assumptions about the shape of the velocity profile [23, 24]. In the following discussion the *xz*-plane will be denoted the vorticity plane and the *xy*-plane the shear plane, whereas the *xz*-plane sometimes in the literature is denoted the shear plane.

Physical Chemistry Chemical Physics Accepted Manuscript

In angular space the Euler equations are applied,

$$\mathbf{I}_p \cdot \dot{\boldsymbol{\omega}}_{pi} = -\boldsymbol{\omega}_{pi} \times \mathbf{I}_p \cdot \boldsymbol{\omega}_{pi} + \boldsymbol{\Gamma}_{pi}, \tag{2.6}$$

where $\mathbf{I}_p$ is the inertia tensor, $\boldsymbol{\omega}_{pi}$ is the angular velocity of molecule *i* and $\boldsymbol{\Gamma}_{pi}$ is the torque exerted on molecule *i* by the other molecules and the subscript '*p*' denotes the principal frame. The relation between the rate of change of the axis vectors of the molecules and the angular velocity is expressed in terms of quaternions [25].

When these equations of motion (2.4)-(2.6) are applied the shear rate dependent viscosity is given by

$$\eta(\gamma) = \lim_{t\to\infty} \langle p_{zx}(t) \rangle_\gamma / \gamma \tag{2.7}$$

where $\langle p_{zx}(t) \rangle_\gamma$ is the *zx*-element of the pressure tensor given by the Irving and Kirkwood expression [26],

$$\mathbf{P} = \left\langle \sum_{i=1}^{N} \frac{\mathbf{p}_i \mathbf{p}_i}{m} - \sum_{i=1}^{N} \sum_{j=i+1}^{N-1} \mathbf{r}_{ij} \mathbf{F}_{ij} \right\rangle_\gamma, \tag{2.8}$$

where $\mathbf{r}_{ij} = \mathbf{r}_j - \mathbf{r}_i$ and $\mathbf{F}_{ij}$ is the force exerted on molecule *i* by molecule *j*. The subscript γ denotes that the averages are evaluated in nonequilibrium ensemble at a finite shear rate. In the Newtonian regime there are seven independent components of the viscosity of a nematic liquid crystal. They can be measured by fixing the director in various angles relative to the stream lines by application of a magnetic or electric field. In this work, however, we will only consider the viscosity that is obtained when no external fields are applied and the director is free to orient relative to the stream lines.Other quantities of interest to characterize the rheological properties are the normal stress differences $\langle p_{zz} - p_{xx} \rangle_\gamma$ and $\langle p_{yy} - p_{zz} \rangle_\gamma$, which are equal to the difference between the pressure in the direction of the velocity gradient and the streaming direction and the difference between the pressure in the rotation direction and direction of the velocity gradient, respectively.

2.3 The alignment angle between the director and the stream lines

A planar Couette velocity field $\mathbf{u} = \gamma z \mathbf{e}_x$ is actually a superposition of one rotational velocity field, $\mathbf{u}_r = (1/2)\gamma(z\mathbf{e}_x - x\mathbf{e}_z)$, corresponding to the symmetric part of the shear rate, $(\nabla \mathbf{u})^s = (1/2)\gamma(\mathbf{e}_z\mathbf{e}_x + \mathbf{e}_x\mathbf{e}_z)$ and one irrotational elongational velocity field,

Physical Chemistry Chemical Physics Accepted Manuscript

$\mathbf{u}_e = (1/2)\gamma(z\mathbf{e}_x + x\mathbf{e}_z)$, corresponding to the antisymmetric part of the shear rate, $(\nabla\mathbf{u})^a = (1/2)\gamma(\mathbf{e}_z\mathbf{e}_x - \mathbf{e}_x\mathbf{e}_z)$, see fig. 1. When an isotropic liquid consisting of non-spherical molecules such as, for example, alkanes, is sheared, there is a linear coupling between the symmetric part of the shear rate and the order tensor [12], since they both are symmetric traceless second rank tensors. Thus there will be a small but finite order parameter even at low shear rates with a corresponding director oriented at 45-degrees relative to the streamlines. It is also possible to think that the elongational part of the velocity field pulls the molecules towards the 45-degree orientation. Since the order parameter is finite the system is in fact a noneequilibrium nematic liquid crystal. Then there will also be a torque exerted by the antisymmetric shear rate on the molecules twisting them towards the streamlines. This torque is very low at low shear rates but it increases with the order parameter, so that the alignment angle decreases with the shear rate. On the other hand, when a nematic liquid crystal is sheared the symmetric traceless part of the shear rate pulls the molecules towards the 45-degree direction. Meanwhile the high order parameter of the liquid crystal means that the torque exerted by the antisymmetric part of the shear rate is very high already at low shear rates, resulting in a compromise where the alignment angle usually falls in an interval between 5 and 30 degrees. The alignment angle is independent of the shear rate in the Newtonian regime and does not change very much in the non-Newtonian regime.

3. Model systems

The model systems in this work are based on the Gay-Berne potential [8, 9],

$$U(\mathbf{r}_{12},\hat{\mathbf{u}}_1,\hat{\mathbf{u}}_2) = 4\varepsilon(\hat{\mathbf{r}}_{12},\hat{\mathbf{u}}_1,\hat{\mathbf{u}}_2)\left[\left(\frac{\sigma_0}{r_{12}-\sigma(\hat{\mathbf{r}}_{12},\hat{\mathbf{u}}_1,\hat{\mathbf{u}}_2)+\sigma_0}\right)^{12} - \left(\frac{\sigma_0}{r_{12}-\sigma(\hat{\mathbf{r}}_{12},\hat{\mathbf{u}}_1,\hat{\mathbf{u}}_2)+\sigma_0}\right)^{6}\right], \qquad (3.1)$$

where $\mathbf{r}_{12} = \mathbf{r}_2 - \mathbf{r}_1$ is the distance vector from the centre of mass of molecule 1 to the centre of mass of molecule 2, $\hat{\mathbf{r}}_{12}$ is the unit vector in the direction of $\mathbf{r}_{12}$ and r_{12} is the length of $\mathbf{r}_{12}$. The parameter σ_0 is the length of the axis perpendicular to the axis revolution, *i.e.* the minor axis of a calamitic ellipsoid of revolution and the major axis of a discotic ellipsoid. The strength and range parameters are given by

$$\varepsilon(\hat{\mathbf{r}}_{12},\hat{\mathbf{u}}_1,\hat{\mathbf{u}}_2) = \varepsilon_0\left[1-\chi^2(\hat{\mathbf{u}}_1\cdot\hat{\mathbf{u}}_2)^2\right]^{-1/2}\left\{1-\frac{\chi'}{2}\left[\frac{(\hat{\mathbf{r}}_{12}\cdot\hat{\mathbf{u}}_1+\hat{\mathbf{r}}_{12}\cdot\hat{\mathbf{u}}_2)^2}{1+\chi'\hat{\mathbf{u}}_1\cdot\hat{\mathbf{u}}_2}+\frac{(\hat{\mathbf{r}}_{12}\cdot\hat{\mathbf{u}}_1-\hat{\mathbf{r}}_{12}\cdot\hat{\mathbf{u}}_2)^2}{1-\chi'\hat{\mathbf{u}}_1\cdot\hat{\mathbf{u}}_2}\right]\right\}^2 \qquad (3.2a)$$

Physical Chemistry Chemical Physics Accepted Manuscript

and

$$\sigma(\hat{\mathbf{r}}_{12},\hat{\mathbf{u}}_1,\hat{\mathbf{u}}_2)=\sigma_0\left\{1-\frac{\chi}{2}\left[\frac{(\hat{\mathbf{r}}_{12}\cdot\hat{\mathbf{u}}_1+\hat{\mathbf{r}}_{12}\cdot\hat{\mathbf{u}}_2)^2}{1+\chi\hat{\mathbf{u}}_1\cdot\hat{\mathbf{u}}_2}+\frac{(\hat{\mathbf{r}}_{12}\cdot\hat{\mathbf{u}}_1-\hat{\mathbf{r}}_{12}\cdot\hat{\mathbf{u}}_2)^2}{1-\chi\hat{\mathbf{u}}_1\cdot\hat{\mathbf{u}}_2}\right]\right\}^{-1/2}, \qquad (3.2b)$$

in which the parameter χ is equal to $(\kappa^2-1)/(\kappa^2+1)$, where κ is the ratio between the axis of revolution and the axis perpendicular to the axis revolution, χ' is equal to $(\kappa'^{1/2}-1)/(\kappa'^{1/2}+1)$, where κ' is the ratio of the potential energy minima of the side-by-side and end-to-end configurations, and ε_0 denotes the depth of the potential minimum in the cross configuration, where $\hat{\mathbf{r}}_{12}$, $\hat{\mathbf{u}}_1$ and $\hat{\mathbf{u}}_2$ are mutually perpendicular. We have also used a purely repulsive version of the Gay-Berne potential [27],

$$U(\mathbf{r}_{12},\hat{\mathbf{u}}_1,\hat{\mathbf{u}}_2)=4\varepsilon(\hat{\mathbf{r}}_{12},\hat{\mathbf{u}}_1,\hat{\mathbf{u}}_2)\left(\frac{\sigma_0}{r_{12}-\sigma(\hat{\mathbf{r}}_{12},\hat{\mathbf{u}}_1,\hat{\mathbf{u}}_2)+\sigma_0}\right)^{18}, \qquad (3.3)$$

where ε and σ are given by equation (3.2) . Since this potential is purely repulsive, there are no potential minima but the value of κ' that has been optimised for the attractive Gay-Berne potential has been retained. This potential is more short-ranged than the ordinary Gay-Berne potential, so that the number of interactions is decreased and the calculations are accelerated. This means that some transport coefficient requiring very long simulations to converge can be evaluated. Since this system to a large extent displays the same phase behaviour as the ordinary Gay-Berne liquid it is still relevant to study it.

More specifically, four model systems (I-IV) have been studied, see table 1. System I is composed of a soft ellipsoid fluid consisting of calamitic ellipsoids interacting according to equation (3.3) with κ equal to 3 and κ' equal to 5 and with the mass m and moment of inertia around the axes perpendicular to the axes of revolution of $I=m\sigma_0^2$. System II is made up by a soft ellipsoid fluid consisting of discotic ellipsoids interacting according to equation (3.3) with κ equal to 1/3 and κ' equal to 1/5, and with the mass m and moment of inertia around the axes perpendicular to the axes of revolution of $I=m\sigma_0^2$. System IIIa is the Memmer model [28] of bent core molecules consisting of two ellipsoids interacting according to equation (3.3) with κ equal to 3 and κ' equal to 5 and with the axes of revolution of the two ellipsoids in the same plane at an angle φ of 140° and a distance of $2\sigma_0\sin\varphi/2\approx 1.88\,\sigma_0$ between the centres of symmetry of the ellipsoids, see fig. 2. The mass is equal to m and the moment of inertia around the axis in the plane of the axes of revolution bisecting the angle φ between

Physical Chemistry Chemical Physics Accepted Manuscript

these axes, I_{zz}, has been set equal to $23\sigma_0^2/18\sin^2(\varphi/2)$, the moment of inertia around the axis perpendicular to the axes of revolution, I_{yy}, has been given the value of $m\sigma_0^2[\sin^2(\varphi/2)+5/18]$ and the moment of inertia around the axis in the plane of the axes of revolution intersecting these axes, I_{xx}, is equal to $5\sigma_0^2\cos^2(\varphi/2)/18$. These expressions for the moment of inertia have been obtained by assuming that the mass in either ellipsoid is concentrated to four equidistant points along the axis of revolution with the mass $m/8$ and spaced apart with a distance of $2\sigma_0/3$. System IIIb is the same as system IIIa but the repulsive potential (3.3) has been replaced by the attractive potential (3.1). Finally, system IV is a soft ellipsoid-string fluid [29] composed of strings of 10 soft discotic ellipsoids of revolution interacting according to equation (3.3) with κ equal to 0.4 and κ' equal to 1/5. The axes of revolution of the ellipsoids are parallel to each other and perpendicular to the line joining their centres of symmetry, see fig. 3. The distance between the centres of symmetry of two adjacent ellipsoids is equal to $0.5\sigma_0$. In this way a non-convex biaxial body is obtained with a length-to-breadth-to-width ratio of 5.5:1:0.4. The mass is equal to *m* and moment of inertia around the axes joining the centres of mass of the ellipsoids, I_{zz}, has been set equal to $m\sigma_0^2/4$ and the moments of inertia around the other two axes, I_{xx} and I_{yy}, have been set equal to $33m\sigma_0^2/16$.

4. Technical details

The quantities in this work are expressed in length, energy, mass and time units of σ_0, ε_0, *m*, the molecular mass, and $\tau=\sigma_0(m/\varepsilon_0)^{1/2}$. Then the units of the pressure, temperature, density, shear rate and viscosity become ε_0/σ_0^3, ε_0/k_B, σ_0^{-3}, τ^{-1} and $\varepsilon_0\tau/\sigma_0^3$, respectively. The equations of motion were integrated by employing a fourth order Gear predictor-corrector method with a timestep of 0.001τ for all the systems except system II, the discotic ellipsoids, where a timestep of 0.0005τ was used. The cut-off radii beyond which the forces and torques were set equal to zero was $4.5\sigma_0$ for the calamitic ellipsoids of systems I and III and to $2.0\sigma_0$ for the discotic ellipsoids of systems II and IV. When system I and II, the calamitic and discotic soft ellipsoids, were simulated 8192 particles were used, when system III, the bent core molecules, were simulated 4096 particles were used and 2025 particles were used to simulate system IV, the soft ellipsoid strings. In order to obtain the viscosity with a relative

Physical Chemistry Chemical Physics Accepted Manuscript

error of less than one percent for shear rates equal to or greater than $0.10\,\tau^{-1}$ it is sufficient to perform simulations with a run length of four million timesteps or less for all the above systems. In order to facilitate the formation of the neighbour list a cell code was used. The expressions for the forces and toques which are rather complicated are given in ref. [30].

5. Calculations, results and discussion

The main topic of this work is to study the shear viscosity and the normal stress differences as functions of the shear rate in the non-Newtonian regime of liquid crystals displaying a nematic phase at equilibrium and to determine whether there is a general form for these functions for a class of systems consisting of rigid calamitic or discotic molecules. In order to find these functions we start by calamitic and discotic soft ellipsoids of revolution since they are the simplest and most regular systems in this class and then we proceed to examine less regular systems such as bent core molecules and finally soft ellipsoid strings that form both uniaxial and biaxial nematic phases.

5.1 Calamitic soft ellipsoids of revolution

At first it is appropriate to illustrate the difference between the functional dependencies of the shear viscosity on the shear rate for liquids that are isotropic at equilibrium and for liquids that are nematic liquid crystals at equilibrium. Therefore, we begin by studying the viscosity of the isotropic phase of the calamitic soft ellipsopids of revolution, system Ia, at a density of $0.20\,\sigma_0^{-3}$, a temperature of $1.00\,\varepsilon_0 / k_B$ and at shear rates between 0.01 and $1.00\,\tau^{-1}$. The results are shown in fig. 4, where the order parameter *S* and the logarithm of the viscosity η are shown as functions of the logarithm of the shear rate γ. At low shear rates in the Newtonian regime the viscosity is constant and then it decreases at the higher shear rates. In the high shear rate limit there is a linear relation between $\log\eta$ and $\log\gamma$, so that there is a power law dependence of the viscosity on the shear rate. This functional dependence is well-known and displayed by alkanes and other non-spherical molecules [3-6]. The reason why the viscosity decreases with the shear rate is that the elongational part of the velocity field, see fig. 1, stretches out the molecules and pulls them towards the 45 degree orientation relative to the stream lines. However, the alignment angle becomes less than 45 degrees at higher shear rates because the rotational part of the velocity field exerts a torque twisting the molecules towards the streamlines, so that the result is compromise leading to an alignment angle of less than 45 degrees. At the highest shear rate it has decreased to 23 degrees, see table I. When the calami-

Physical Chemistry Chemical Physics Accepted Manuscript

tic molecules are aligned in this way, there will be fewer side-by-side collisions in the direction of the streamlines so that the friction and thereby the viscosity decreases. This decrease is directly reflected by the dependence of the order parameter on the shear rate. It is zero in the Newtonian regime and then it increases more or less linearly with the logarithm of the shear rate at high shear rates. Thus the shear field transforms the isotropic system to a nonequilibrium nematic liquid crystal.

If we increase the density to $0.30\,\sigma_0^{-3}$ we enter the nematic equilibrium phase. The viscosity as a function of the shear rate is shown in fig. 5a, where it can be seen that the viscosity dependence on the shear rate has changed – it turns out the liquid still is shear thinning and that the logarithm of the viscosity to a good approximation is a linear function of the square root of the shear rate or that the viscosity itself is proportional to an exponential function of the square root of the shear rate in the non-Newtonian regime. This functional dependence starts at lower shear rates than the asymptotic power law in the isotropic phase and it is valid up to the highest shear rates. This is similar to the behaviour of Lennard-Jones liquids and WCA-liquids [2] even though it is the viscosity itself that is a linear function of the square root of the shear rate in those systems. The decrease of the viscosity with the shear rate in the nematic phase can be attributed to the increasing order parameter even though this parameter is rather high, *i.e.* 0.75, already at equilibrium. However, the order parameter still increases with the shear rate due to the coupling between the symmetric traceless part of the shear rate and the order tensor, and it is a linear function of the square root of shear rate at low and intermediate shear rates. It could also be thought that the decrease of the viscosity is due to a decreasing alignment angle, so that the molecules would become closer to the streamlines. However, this is not the case, since it is almost constant and independent of the shear rate and it even increases slightly with the shear rate, *i.e.* from 20 degrees at equilibrium to 22 degrees at the highest shear rates, see table 1.

Finally, it should be acknowledged that it was found that the original Gay-Berne liquid was shear thinning in ref. 11, however, the actual functional dependence of the viscosity on the shear rate was not discussed there.

5.2 Discotic soft ellipsoids of revolution

In order to determine whether the above shear rate dependence of the viscosity in the nematic phase is a peculiarity of liquids consisting of calamitic soft ellipsoids of revolution, we continue to examine a liquid composed of the discotic soft ellipsoids of revolution at a

Physical Chemistry Chemical Physics Accepted Manuscript

density of $2.4\,\sigma_0^{-3}$ and a temperature of $1.00\ \varepsilon_0 / k_B$, where the equilibrium phase is nematic, system II. In this case it is found that the logarithm of the viscosity is an approximately linear function of the square root of the shear rate too and the order parameter itself is a linear function of the square root of the shear rate at low to intermediate shear rates and then levels off at the higher shear rates, see fig. 5b. Thus the viscosities of calamitic and discotic soft ellipsoids display a similar functional dependence on the shear rate in the nematic phase.

5.3 Bent core molecules

Both of the two above systems consist of very regular and convex symmetric ellipsoids of revolution so that it could still be argued that the approximately linear dependence of the logarithm of the viscosity on the square root of the shear rate is a special feature limited to these systems. Therefore we continued to investigate systems consisting of bent core molecules. In fig. 5c we show the viscosity and the order parameter of a nematic phase of such molecules consisting of two repulsive soft ellipsoids, system IIIa, at a density of $0.17\,\sigma_0^{-3}$, where the equilibrium phase is nematic. Also here $\log\eta$ is a linear function of $\gamma^{1/2}$. Note that the viscosity continues decreasing at the high shear rates when the order parameter has levelled off and is independent of the shear rate. The Newtonian behaviour at low shear rates is hard to observe because the signal-to-noise ratio becomes very low in this shear rates regime.

In the systems studied so far, the intermolecular interaction potentials are purely repulsive, which means that they can be regarded as a high temperature limit. Therefore, the effect of attraction was tested by including a study of the viscosity of a system consisting of bent core molecules interacting according to the original attractive Gay-Berne potential at a density of $0.18\,\sigma_0^{-3}$ and a temperature of $1.5\,\varepsilon_0 / k_B$, system IIIb, where a nematic phase is found at equilibrium. Also here $\log\eta$ is a linear function of $\gamma^{1/2}$, see fig. 5d, and the viscosity continues decreasing at high shear rates even though the order parameter is constant.

We can consequently draw the conclusion that the viscosity is an approximately exponential function of the square root of the shear rate for a large class of nematic equilibrium phases consisting of rigid calamitic or discotic molecules and that this functional dependence is not limited to convex molecules with axial symmetry.

Physical Chemistry Chemical Physics Accepted Manuscript

5.4 Biaxial nematic liquid crystals

We finish with a study of a system consisting of soft ellipsoid strings composed of ten discotic ellipsoids the axes of revolution of which are parallel to each other and perpendicular to the line joining their centres of symmetry, see fig. 3. Thus a non-convex biaxial body is obtained. The phase diagram of this system has been comprehensively studied in ref. [29] and it displays isotropic, uniaxial nematic and biaxial nematic phases. At a density of $0.16\,\sigma_0^{-3}$ and a temperature of $1.00\,\varepsilon_0 / k_B$, a uniaxial nematic phase is present at equilibrium and if the density is raised to $0.20\ \sigma_0^{-3}$ while the temperature still is equal to $1.00\,\varepsilon_0 / k_B$, a biaxial nematic equilibrium phase is formed. The viscosity and the uniaxial order parameter as functions of the shear rate are displayed in figs. 5e and 5f. It is obvious that even in these cases the logarithm of the viscosity is a linear function of the square root of the shear rate to a good approximation and thus behaves in the same way as the corresponding functions of the liquids consisting of the calamitic and discotic ellipsoids and of the bent core molecules. The order parameter increases with the shear rate over the whole shear rate interval studied.

Thus this shear rate dependence of the viscosity in the nematic phase is very distinct for all the systems studied. It is also interesting that it starts at lower shear rates than the power law dependence found for the liquids that are isotropic at equilibrium, where it is an asymptotic dependence at high shear rates. This should make it easier to observe the former dependence experimentally. Substances likely to display this behaviour are *p*-quinquephenyl and *p*-azoxyanisole, which are composed of rather rigid calamitic cores.

5.5 Normal stress differences

Two other quantities that are useful for the characterisation of rheological properties are the two normal stress differences $\langle p_{zz} - p_{xx} \rangle_\gamma$ and $\langle p_{yy} - p_{zz} \rangle_\gamma$ as functions of the shear rate, where the first quantity is the difference between the normal pressures in the direction of the velocity gradient and in the direction of the streamlines, and the second quantity is the difference between the normal pressure in the direction perpendicular to the vorticity plane and in the direction of the velocity gradient. The normal stress differences behave differently in phases that are isotropic and nematic at equilibrium, respectively. Therefore, we begin by examining them for the calamitic soft ellipsopids of revolution at a density of $0.20\,\sigma_0^{-3}$, a temperature of $1.00\,\varepsilon_0 / k_B$, system Ia. The results are shown in fig. 6, where it can be seen that there is an approximately parabolic dependence of the normal stress difference on shear rate

Physical Chemistry Chemical Physics Accepted Manuscript

and that their derivative s with respect to the shear rate goes to zero as the shear rate goes to zero and. In fig. 7 they are shown for the calamitic soft ellipsopids of revolution, at a density of $0.30\,\sigma_0^{-3}$, a temperature of $1.00\,\varepsilon_0 / k_B$, system Ib, in the nematic phase. Here the normal stress differences are linear functions of the shear rate at low to intermediate shear rates and then they level off slightly at the highest shear rates.

This difference of the functional dependence of the normal stress differences on the shear rate is related to the symmetry of the systems. In the isotropic phase in the Newtonian regime the shear rate is the *zx*-element of the strain rate tensor and it can couple only with the shear stress which is the *zx*-element of the stress tensor. It cannot couple with the normal stress differences which are diagonal elements of the stress tensor, so that the normal stress differences must remain zero there. When the shear rate increases the order parameter increases from zero, so that the system becomes a non-equilibrium nematic liquid crystal where the shear rate is allowed couple to normal stress differences, so that the normal stress differences will gradually increase from zero. On the other hand, in system Ib being nematic at equilibrium, there is a linear relationship between the normal stress differences and the shear rate already in the Newtonian regime [17, 18, 31, 32], so that the normal stress differences are proportional to the shear rate even at low shear rates and this linear relation apparently persists up to intermediate shear rates. At the highest shear rates the normal stress differences level off. As a consequence of the symmetry the functional relationship between the normal stress differences and the shear rate is similar for all the nematic systems studied. The relationship can be represented by a parabolic curve fit given in table 2. Note that $\langle p_{zz} - p_{xx} \rangle_\gamma$ is positive and that the quadratic term of the parabolic curve fit is negative for all the systems studied, so that this component levels off at high shear rates. On the other hand, $\langle p_{yy} - p_{zz} \rangle_\gamma$ is negative and the quadratic term of the parabolic curve fit is positive for all the systems studied, so that the absolute magnitude of this component also levels off at high shear rates. This means that the pressure in the z-direction or in the direction of the velocity gradient is larger than the pressure in the directions of the streamlines and in the direction perpendicular to the vorticity plane when the liquid is sheared.

6. Conclusion

We have calculated the viscosity and the normal stress differences as functions of the shear rate of molecular models systems consisting of rigid calamitic or discotic molecules

Physical Chemistry Chemical Physics Accepted Manuscript

interacting according to various versions of the Gay-Berne potential in order to determine whether these functions attain a general form for these systems. More specifically, four different systems were studied: calamitic soft purely repulsive ellipsoids (I), discotic soft purely repulsive ellipsoids (II), bent core molecules consisting of two soft purely repulsive ellipsoids arranged at an angle relative to each other (IIIa) and of two soft ellipsoids arranged at an angle relative to each other interacting via the original attractive Gay-Berne potential (IIIb) and finally a system consisting of the soft ellipsoid strings, *i.e*. a string of ten purely repulsive soft discotic ellipsoids of revolution, the axes of which are parallel to each other and perpendicular to the line joining their centres of symmetry (IV). This last system forms uniaxial and biaxial nematic phases at equilibrium.

It was found that the viscosity of the isotropic equilibrium phases behaves like the viscosity of other non-spherical molecules under shear, namely that there is a Newtonian regime at low shear rates where the viscosity is constant and independent of the shear rate followed by an asymptotic shear thinning regime at high shear rates where the viscosity follows a power law, *i. e*. the viscosity is proportional to the shear rate raised to a power. The shear thinning is due to the shear induced alignment of the molecules whereby a non-equilibrium liquid crystal is formed with a director close to the stream lines. Thereby the molecule can pass each other more readily, so that the friction decreases.

When the nematic equilibrium phases were sheared, it was found, for of all the above systems, that they are shear thinning and that the logarithm of the viscosity is an approximately linear function of the square root of the shear rate. This shear thinning, which is somewhat unexpected since the molecular alignment is very high already at equilibrium, can be attributed to the increasing order parameter, which continues increasing with the shear rate up to very high shear rates. It could be imagined that the alignment angle between the director and the stream lines should decrease with the shear rate and that this would contribute to the decrease of the viscosity but this is not the case - the alignment angle is rather constant in the non-Newtonian regime and there is even a slight increase.

The normal stress differences are equal to zero in Newtonian regime in the isotropic phases due to symmetry restrictions and increase in a parabolic fashion at higher shear rates where the isotropic liquid has been transformed to a non-equilibrium liquid crystal. In the nematic phase on the other hand, there is a linear relation between the shear rate and the normal stress differences given by symmetry in the Newtonian regime. It was found that this linear relation persists for all of the above systems up to intermediate shear rates and that it levels.

Physical Chemistry Chemical Physics Accepted Manuscript

Acknowledgement

We gratefully acknowledge financial support from the Knut and Alice Wallenberg Foundation (Project number KAW 2012.0078) and Vetenskapsrådet (Swedish Research Council) (Project number 2013-5171). The simulations were performed using resources provided by the Swedish National Infrastructure for Computing (SNIC) at PDC, HPC2N and NSC.).

Physical Chemistry Chemical Physics Accepted Manuscript

REFERENCES

1. A. W. Lees and S. F. Edwards, J. Phys., 1972, **C 5**, 1921.
2. D. J. Evans and G. P. Morriss, Statistical Mechanics of Nonequilibrium Liquids, Academic Press, London, 1990.
3 R. Edberg, D. J. Evans and G. P. Morriss, J. Chem. Phys., 1987, **86**, 4555.
4. G. P. Morriss, P. J. Daivis and D. J. Evans, J. Chem. Phys., 1991, **94**, 7420.
5. P. J. Daivis, D. J. Evans and G. P. Morriss, J. Chem. Phys., 1992, **97**, 616.
6. J. D. Moore, S. T. Cui, H. D. Cochrane and P. T. Cummings, J. Chem. Phys., 2000, **113**, 8833.
7. J. C. Maxwell, Proc. R. Soc. London, Ser. A, 1873, **22**, 151.
8. J. G. Gay and B. J. Berne, J. Chem. Phys., 1981, **74**, 3316.
9. M. A. Bates and G. R. Luckhurst, J. Chem. Phys., 1996, **104**, 6696.
10. I. Cacelli, G. Prampolini, and A. Tani, J. Phys. Chem. B*,* 2005, **109***,* 3531.
11. N. Mori, J. Morimoto and K. Nakamura, Mol. Cryst. Liq. Cryst., 1997, **307**, 15.
12. S. Sarman and D. J. Evans, J. Chem. Phys., 1993, **99**, 9021.
13. L. de Gaetani, G. Prampolini, and A. Tani, J. Phys. Chem. B, 2006, **110**, 2847.
14. D. Baalss and S. Hess, Phys. Rev. Lett., 1986, **57**, 86.
15. D. Baalss and S. Hess, *Z.* Naturforsch. A: Phys. Sci., 1988, **43**, 662.
16. S. Sarman and A. Laaksonen, J. Comput. Theor. Nanosci., 2011, **8**, 1081.
17. S. Chandrasekhar, Liquid Crystals, Cambridge University Press, Cambridge, 1992.
18. P. G. DeGennes and J. Prost, The Physics of Liquid Crystals, Clarendon Press, Oxford, 1992.
19. C. Bailey, K. Fodor-Csorba, J. T. Gleeson, S. N. Sprunt and A. Jakli, Soft Matter, 2010, **6**, 1704.
20. E. Dorjgotov, K. Fodor-Csorba, J. T. Gleeson, S. Sprunt and A. Jáklia, Liquid Crystals, **35**, 2008, 149.
21. R. Eidenschink, US Pat., 5 160 451, 1992.
22. R. Eidenschink and H. Kretzschmann, PCT application, WO065785, 2009.
23. K. P. Travis, P. J. Daivis, and D. J. Evans, J. Chem. Phys., 1995, **103**, 1109.
24. K. P. Travis, P. J. Daivis, and D. J. Evans, J. Chem. Phys., 1995, **103**, 10638.
25. D. J. Evans, Mol. Phys., 1977, **34**, 317.
26. H. Irving and J. G. Kirkwood, J. Chem. Phys., 1950, **18**, 817.
27. S. Sarman, J. Chem. Phys., 1994, **101**, 480.
28. R. Memmer, Liquid Crystals, 2002, **29**, 483.

Physical Chemistry Chemical Physics Accepted Manuscript

29. S. Sarman, Phys. Chem. Chem. Phys., 2000, **2**, 3831.
30. S. Sarman and D. J. Evans, J. Chem. Phys., 1993, **99**, 620.
31. Hess, J. Non-Equilib. Thermodyn., 1986, **11**, 175.
32. S. Sarman, J. Chem. Phys., 1995, **103**, 393.

Physical Chemistry Chemical Physics Accepted Manuscript

TABLES

Table 1

System	Interaction potential	Equilibrium phase	$n\sigma_0^3$	$k_B T / \varepsilon_0$	θ
Ia	calamitic soft ellipsoid	isotropic	0.20	1.00	45-23
Ib	calamitic soft ellipsoid	uniaxial nematic	0.30	1.00	20-22
II	discotic soft ellipsoid	uniaxial nematic	2.40	1.00	111-112
IIIa	bent core soft ellipsoid	uniaxial nematic	0.17	1.00	8-11
IIIb	bent core attractive ellipsoid	uniaxial nematic	0.18	1.50	3-10
IVa	soft ellipsoid string	uniaxial nematic	0.16	1.00	7-6
IVb	soft ellipsoid string	biaxial nematic	0.20	1.00	1-5

Table 2

System	a_1	b_1	c_1	a_2	b_2	c_2
Ib	0.009	1.886	-0.540	0.000	-1,031	0.130
II	0.018	8.207	-1.752	-0.010	-3.225	0.200
IIIa	0.016	3.010	-1.760	-0.003	-1.152	0.527
IIIb	-0.024	1.661	-0.373	0.009	-0.681	0.113
IVa	0.000	0.310	-0.048	0.000	-0.082	0.007
IVb	-0.004	0.498	-0.064	0.000	-0.010	0.007

Physical Chemistry Chemical Physics Accepted Manuscript

FIGURE CAPTIONS

Fig. 1

The shear velocity field $\mathbf{u} = \gamma z \mathbf{e}_x$ is a sum of a rotational velocity field, $\mathbf{u}_r = (1/2)\gamma(z\mathbf{e}_x - x\mathbf{e}_z)$, and an irrotational elongational velocity field, $\mathbf{u}_e = (1/2)\gamma(z\mathbf{e}_x + x\mathbf{e}_z)$.

Fig. 2

The bent core molecule is composed of two ellipsoids, the axes of revolution of which lie in the same plane. The angle between these axes is denoted by φ. In the principal coordinate system the $\boldsymbol{x}_p$ -axis passes through the centre of symmetry of either ellipsoid, the $\boldsymbol{y}_p$ -axis is perpendicular to the plane of the axes of revolution and the $\boldsymbol{z}_p$ -axis lies in the same plane as these two axes and bisects the angle between them.

Fig. 3

The molecules of the soft ellipsoid-strings consist of a linear string of discotic soft ellipsoids of revolution, the symmetry axes of which are parallel to each other and perpendicular to the line joining their centres of mass. The principal axes are denoted by $\boldsymbol{x}_p$ parallel to the line through the centres of mass, $\boldsymbol{z}_p$ parallel to the symmetry axes of the ellipsoids and $\boldsymbol{y}_p = \boldsymbol{z}_p \times \boldsymbol{x}_p$ (a) Projection perpendicular to the $\boldsymbol{z}_p$ -axis (b) Projection perpendicular to the $\boldsymbol{y}_p$ -axis

Fig. 4

The viscosity η (left hand axis, filled squares) and the order parameter S (right hand axis, open diamonds) of the fluid consisting of calamitic soft ellipsoids as a function of the shear rate γ, in the phase that is isotropic at equilibrium at a density of $0.20\,\sigma_0^{-3}$ and a temperature of $1.00\,k_B T / \varepsilon_0$, system Ia. The error bars are of the size of the symbols.

Fig. 5a

The viscosity η (left hand axis, filled squares) and the order parameter S (right hand axis, open diamonds) of the fluid consisting of calamitic soft ellipsoids as a function of the

Physical Chemistry Chemical Physics Accepted Manuscript

shear rate γ, in a phase that is nematic at equilibrium at a density of $0.30\,\sigma_0^{-3}$ and a temperature of $1.00\,k_BT/\varepsilon_0$, system Ib. The error bars are of the size of the symbols.

Fig. 5b

The viscosity η (left hand axis, filled squares) and the order parameter S (right hand axis, open diamonds) of the fluid consisting of discotic soft ellipsoids as a function of the shear rate γ, in a phase that is nematic at equilibrium at a density of $2.40\,\sigma_0^{-3}$ and a temperature of $1.00\,k_BT/\varepsilon_0$, system II. The error bars are of the size of the symbols.

Fig. 5c

The viscosity η (left hand axis, filled squares) and the order parameter S (right hand axis, open diamonds) of the fluid consisting of bent core molecules composed of two calamitic soft ellipsoids, as a function of the shear rate γ in the nematic phase at a density of $0.17\,\sigma_0^{-3}$ and a temperature of $1.00\,k_BT/\varepsilon_0$, system IIIa. The error bars are of the size of the symbols.

Fig. 5d

The viscosity η (left hand axis, filled squares) and the order parameter S (right hand axis, open diamonds) of the fluid consisting of bent core molecules composed of two calamitic attractive Gay-Berne ellipsoids as a function of the shear rate γ in the nematic phase at a density of $0.18\,\sigma_0^{-3}$ and a temperature of $1.50, k_BT/\varepsilon_0$, system IIIb. The error bars are of the size of the symbols.

Fig. 5e

The viscosity η (left hand axis, filled squares) and the order parameter S (right hand axis, open diamonds) of the soft ellipsoid strings, system IVa as a function of the shear rate γ in the uniaxial nematic phase at a density of $0.16\,\sigma_0^{-3}$ and a temperature of $1.00\,k_BT/\varepsilon_0$. The error bars are of the size of the symbols.

Fig. 5f

As in fig. 11 but the density is equal to of $0.20\,\sigma_0^{-3}$ and the equilibrium phase is a biaxial nematic phase, system IVb.

Physical Chemistry Chemical Physics Accepted Manuscript

Fig. 6

The normal stress differences $\langle p_{zz} - p_{xx} \rangle_\gamma$ (filled squares) and $\langle p_{zz} - p_{yy} \rangle_\gamma$ (diamonds) of the fluid consisting of calamitic soft ellipsoids as a function of the shear rate γ a density of $0.20\,\sigma_0^{-3}$ and a temperature of $1.00\,k_B T / \varepsilon_0$, system Ia. The error bars are of the size of the symbols.

Fig. 7

As in fig. 2 but the density is equal to $0.30\,\sigma_0^{-3}$ and the phase is nematic at equilibrium system Ib.

Physical Chemistry Chemical Physics Accepted Manuscript

Table captions

Table 1

The various systems and state point studied. The last column is the interval of the alignment angle θ over the studied shear rate ranges.

Table 2

Curve fits of the normal stress differences of the nematic phase as functions of the shear rate to second degree polynomials, $\langle p_{zz} - p_{xx} \rangle_\gamma = a_1 + b_1\gamma + c_1\gamma^2$ and $\langle p_{yy} - p_{zz} \rangle_\gamma = a_2 + b_2\gamma + c_2\gamma^2$. In all the cases the correlation coefficient is equal to 1.00.

Physical Chemistry Chemical Physics Accepted Manuscript

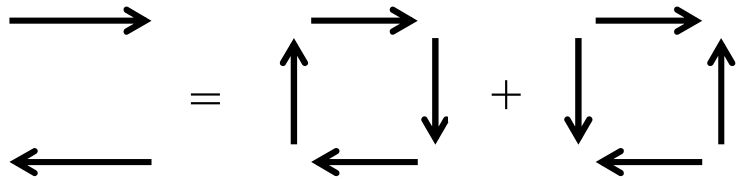

Fig 1.

Physical Chemistry Chemical Physics Accepted Manuscript

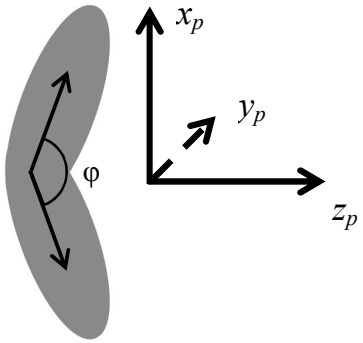

Physical Chemistry Chemical Physics Accepted Manuscript

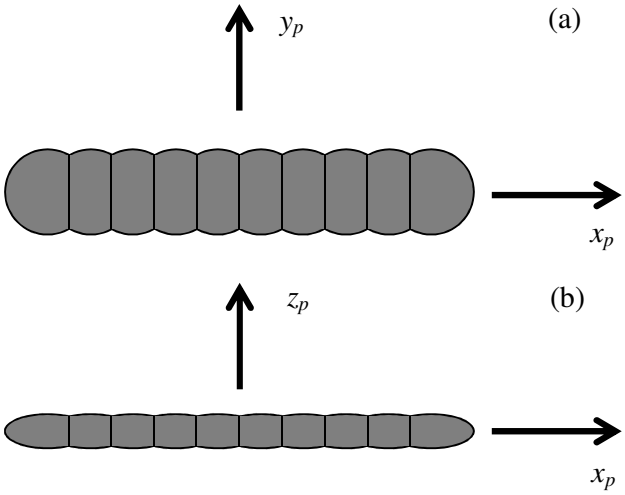

Physical Chemistry Chemical Physics Accepted Manuscript

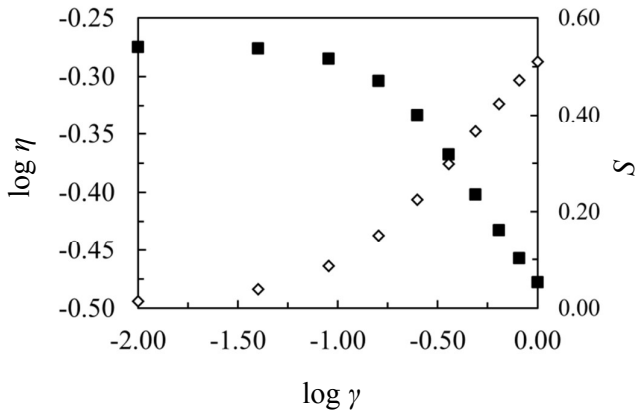

Fig. 4

Physical Chemistry Chemical Physics Accepted Manuscript

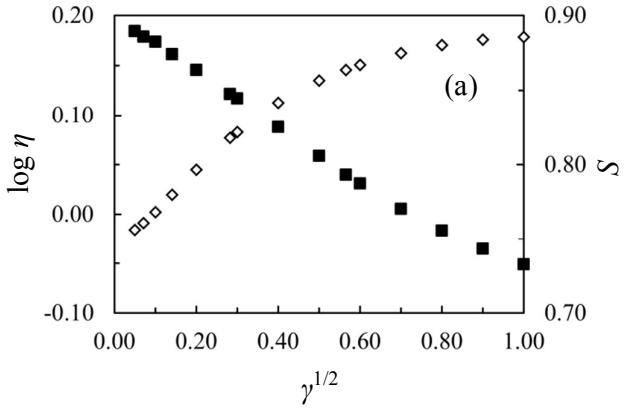

Fig. 5a

Physical Chemistry Chemical Physics Accepted Manuscript

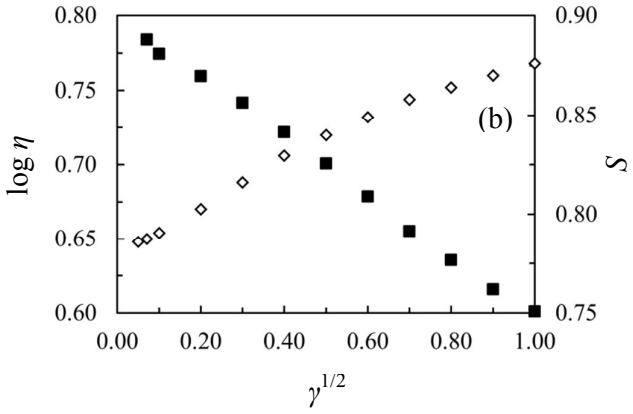

Fig. 5b

Physical Chemistry Chemical Physics Accepted Manuscript

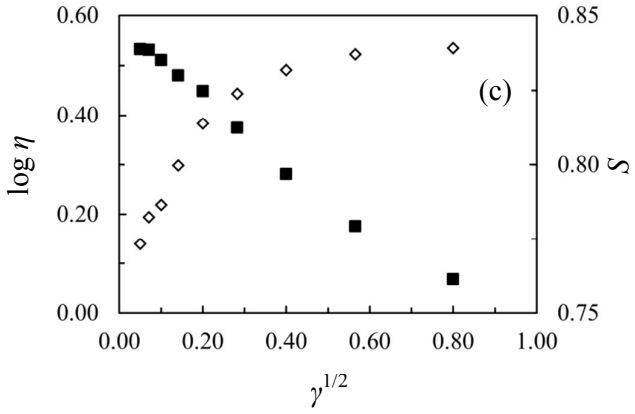

Fig. 5c

Physical Chemistry Chemical Physics Accepted Manuscript

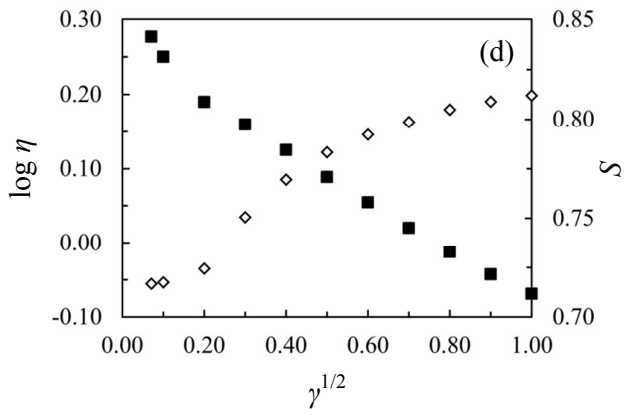

Fig. 5d

Physical Chemistry Chemical Physics Accepted Manuscript

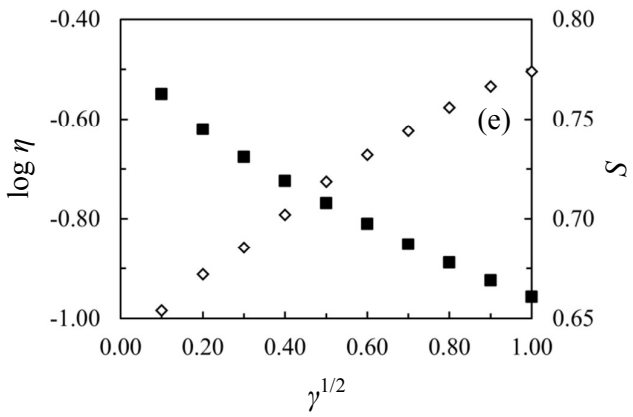

Fig. 5e

Physical Chemistry Chemical Physics Accepted Manuscript

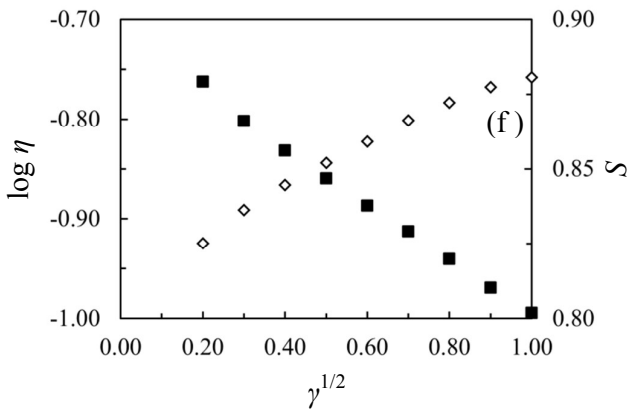

Fig. 5f

Physical Chemistry Chemical Physics Accepted Manuscript

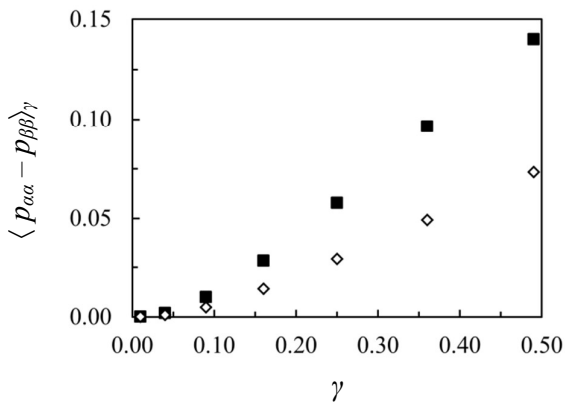

Fig. 6

Physical Chemistry Chemical Physics Accepted Manuscript

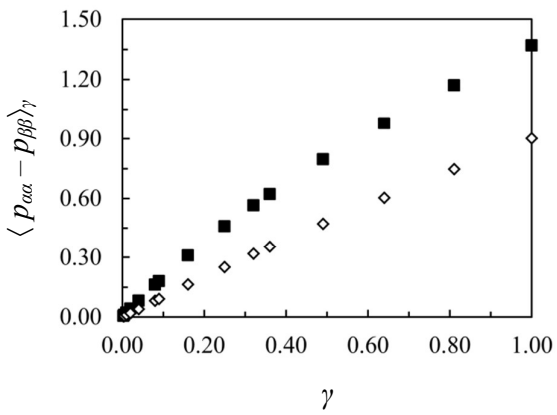

Fig. 7

Physical Chemistry Chemical Physics Accepted Manuscript